5.3

ADVANTAGES OF A COORDINATED SCANNING DOPPLER LIDAR AND CLOUD RADAR SYSTEM FOR WIND MEASUREMENTS

K. Träumner[1], J. Handwerker, A. Wieser, J. Grenzhäuser and Ch. Kottmeierr

Institut für Meteorologie und Klimaforschung

Karlsruhe Institute of Technology, Karlsruhe, Germany

During the COPS field campaign a $2\ \mu m$ Doppler lidar and a 35.5 GHz cloud radar were collocated. Due to the different wavelengths, the scattering properties of the particles seen by the two instruments differ. It is shown, that the fraction of horizontal wind profile availibility in the lowest 2 km above ground based on lidar is 32% and increased to 50.6% by additional radar data. Vertical profiles of the horizontal wind can be extended using a combined system. Measuring vertical velocities in vertical stare mode with both systems resulted partly in different velocities obtained from lidar and radar, which is explained by size-dependent terminal fall velocities. Double peaks are detected in the Doppler-spectra of lidar during rain events, which can be related to motion of aerosols and falling droplets. Different measured velocities of falling droplets by lidar and radar are used to gain approximate information about the size distribution of the scatterers. On clear air days velocity differences are not observed and calculated power spectra agreed well within the frequency range from 10^{-4} Hz to $2 \cdot 10^{-2}$ Hz.

1 Introduction

Active remote sensing techiques by radar and lidar are well-established methods for probing the atmosphere. New commercially available small and transportable scanning lidar and radar systems, operating eye save and fully automated, allow new measurement approaches. We present a study using a $2\ \mu m$ lidar and a 35.5 GHz radar. Coordinated simultaneous measurements within the same volume of air using different systems deliver independent and complementary information about the scatterers, among others about their velocity. We investigate occurring differences in velocity measurements from these two systems and the potential to use them to obtain profiles of the horizontal and vertical wind over an extended height range.

2 Instrumental and experimental setup

The instrument combination consists of two 2-axes-scanning remote-sensing systems. Both are able to measure the line-of-sight velocity using the Doppler effect caused by the motion of the scatterers. The lidar is a $2\ \mu m$ Windtracer Systems produced by Lockheed Martin Coherent Technologies. The cloud radar is also a commercial available system of type MIRA36-S with a wavelength of 35.5 GHz. Table 1 summarizes the properties of the two instruments.

During the COPS measurement campaign (Convective and Orographically-induced Precipitation Study, Wulfmeyer et al., 2008) from June to August 2007 the two instruments were collocated on Hornisgrinde mountain in the Black Forest. They both were part of a coordinated scan strategy optimized to get best synergetic measurement data together with a Rotational Raman lidar and a DIAL. The scan strategy consisted of different scenarios depending on the meteorological situation. The scan scenarios were not optimized for instrument intercomparison, but the data set provided a wide range of different measurement situations to analyze the advantages of a combined measurement system.

3 Horizontal wind measurements

Profiles of horizontal wind velocity and direction are a standard information needed in meteorological research. Assuming that the aerosol in the atmosphere drifts with the horizontal wind independent of particle size, the two instruments should deliver same results. Horizontal wind cannot be measured directly, but has to be determined from several measurements with different azimuth angles. For the cloud radar an improved VAD algorithm was applied to all available PPI scans at $75°$ elevation (Handwerker and Görsdorf, 2006). For the lidar velocity, data during 10 minute intervals (containing two PPI scans at $4°$ and $45°$ elevation and four RHI scans at different azimuth angles) was collected and grouped into cylindric slices of 50 m height and 2000 m radius. A fitting algorithm analog to VAD algorithm (Browning and Wexler, 1968) was used to calculate the u and v components minimizing the root-mean-square sum. This procedure has the advantage that more data points are used for calculation, the drawback is the lower temporal resolution compared to use each PPI. For each height a quality index was calculated from the root-mean-square difference between the measured and the fitted line-of-sight velocity. Horizontal wind data below $5\ ms^{-1}$ with an absolute error of more than $1\ ms^{-1}$ and data above $5\ ms^{-1}$ with a relative error of 20% are neglected.

The radar provided 1801 vertical profiles of horizontal wind during COPS. Due to a different scan pattern applied in June, the lidar got 3249 vertical profiles over the hole period. 1268 profiles have been measured si-

---
[1]Corresponding author address: Katja Träumner, Institut für Meteorologie und Klimaforschung, Forschungszentrum Karlsruhe, Hermann-Von-Helmholtz-Platz 1, 76344 Eggenstein-Leopoldshafen, Germany; email: katja.traeumner@imk.fzk.de

Table 1: instrument specifications

	cloud radar	wind lidar
wavelength	8.44 mm	2.023 μm
pulse width	200 ns	425 ns
pulse repetition frequency	5 kHz	500 Hz
unambiguous velocity	$\pm 10.6\ ms^{-1}$	$\pm 20\ ms^{-1}$
sampling rate	50 MHz	100 MHz
peak power	30 kW	4.5 kW
range gates	512	100
lowest range gate	150 m	350 m
spatial resolution	30 m	72 m
azimuth angle	-3 ... 363°	0 ... 360°
elevation angle	45 ... 135°	-5 ... 185°
scan velocity	up to $10°s^{-1}$	$0.1 ... 25°s^{-1}$

multaneously, but only 71% of the profiles could be used for further investigation, restricted by missing appropriate scatterers. This is equivalent to 151 measurement hours. Different height levels are adjusted by averaging the data in 50 m height intervals. For the total of all time-height intervals from the ground up to $8\ km$ height, radar data are available during 17%, lidar data during 9% and simultaneously measured data during 3%. The low lidar data amount resulted from the low aerosol concentrations above the atmospheric boundary layer. Within the lowest 2 km above ground, relevant for boundary layer research, lidar data are available during 32%, radar data during 28% and both instruments measured simultaneously during 9% of all time-height intervals. Thus a combination of both instruments yields to an increase of available information from 32% up to 51%. Further simultaneous data of the both instruments are rare. This is not a drawback, but shows the potential and need of combining the instruments.

Figure 1 shows all the simultaneously measured data points. The velocities in the lowest 2 km above ground (blue) agree within less than $1\ ms^{-1}$ in 45% of data, 13% differed by more than $5\ ms^{-1}$. The difference in wind direction was smaller than 10° in 50% and larger than 45° in 13%. Considering the height up to 8 km (red) the values differed slightly.

Figure 1 frequently shows small radar velocities between 0 and $3\ ms^{-1}$ whereas lidar velocities are up to $20\ ms^{-1}$. This effect results from a ground clutter problem of the cloud radar, which received signals from stagnant objects. After identifying this problem a closer look at the radar data showed, that ground clutter echoes could be identified by a low spectral width as well. After correcting the radar data for ground clutter and recalculating the horizontal wind speed and direction, this problem vanished (Figure 2).

The fraction of velocities differing by less than $1\ ms^{-1}$ increases to 55% and the amount of data differing more than $5\ ms^{-1}$ is reduced to only 3%. The fraction of wind direction data differing by more than

45° drops to 5%. This clearly shows, that the combination of the two instruments allows to identify and to correct for measurement errors, which are not detectable using only one instrument.

As mentioned above an important advantage of the instrument combination is to extend the wind information. Due to the different wavelengths, the cloud radar and the lidar experience appropriate scattering during different atmospheric situations. This leads to an extension of the wind information in time, e.g. by changing weather situations from clear air lidar optimal weather to cloudy radar weather, and in space, due to complementation in height. During COPS clear air days with high humidity and days with small cumulus convection showed good conditions for both instruments, whereas clear air days with dry conditions were favorable for lidar measurements and days with low cloud base or fog were favorable for the radar. Characteristic profiles for different situations are shown in Figure 3.

4 Vertical wind measurements

Vertical scatterer velocities are no longer independent of scatterers size. Especially the larger aerosols have a size dependent terminal fall velocity. Due to the different wavelengths of the radar (8.5 mm) and the lidar ($2\ \mu$m), the instruments are sensitive to scatterers of different sizes. Following the theory of Rayleigh scattering for the radar and optical scattering for lidar, which is reasonable for aerosols larger than $5\ \mu m$, size distribution dependent velocities result as:

$$v_{Radar} = \frac{\int v(D)dZ}{\int dZ} \tag{1}$$

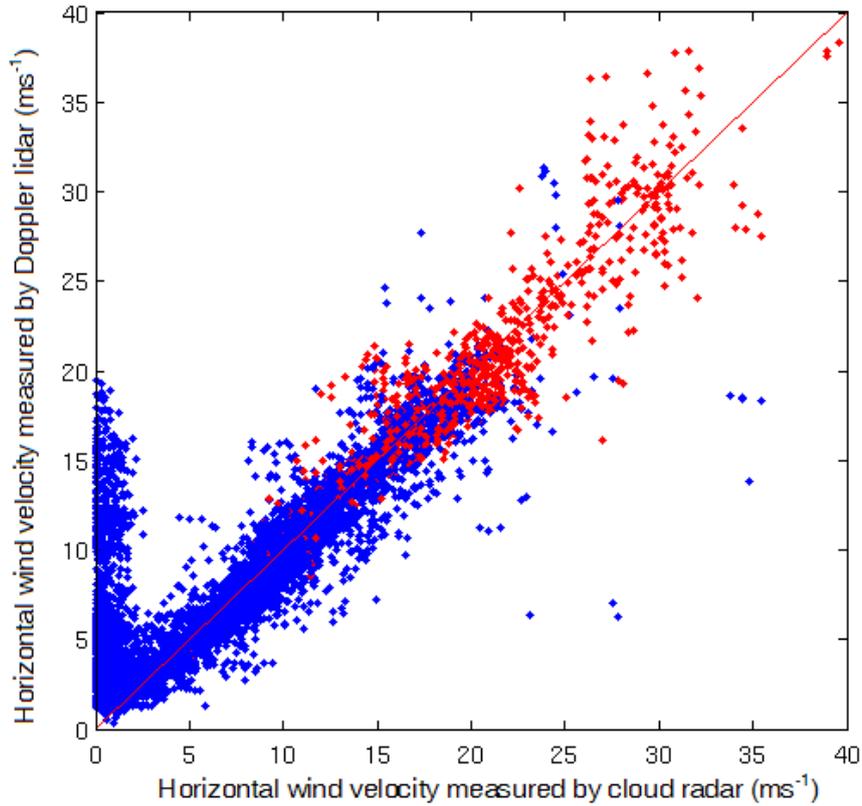$$= \frac{\int v(D) \cdot N(D) \cdot D^6 dD}{\int N(D) \cdot D^6 dD} \tag{2}$$

Figure 1: Simultaneously measured horizontal wind velocity in the lowest 2 km above ground (blue) and from 2 to 8 km above ground (red).

$$v_{Lidar} \quad = \quad \frac{\int v(D)dB}{\int dB} \qquad (3)$$

$$= \quad \frac{\int v(D) \cdot N(D) \cdot D^2 dD}{\int N(D) \cdot D^2 dD} \qquad (4)$$

with scatterer radius D, velocity of the scatterer $v(D)$ dependent on D, radar reflectivity Z, lidar backscatter coefficient B and number density of the scatterer N.

Vertical wind velocities are measured directly in vertical-stare-mode. During COPS the cloud radar measured with a temporal resolution of 0.1 Hz and a spatial resolution of 30 m, the lidar with 1 Hz and 72 m. For both instruments a small velocity bias could be excluded by former measurements. Temporal averaging was performed for lidar data and spatial averaging for radar data to get comparable range gates. Regarding the vertical range from 400 to 7500 m agl over the complete COPS period, the radar delivered twice the amount of valid data compared to the lidar. Reducing the vertical extend to the lowest 2 km above ground the two instruments showed about the same amount of valid data. The amount of useful data could be increased by a factor of 1.7 in the lowest 2 km by merging data compared to single lidar measurements. The data from all simultaneously measured range gates
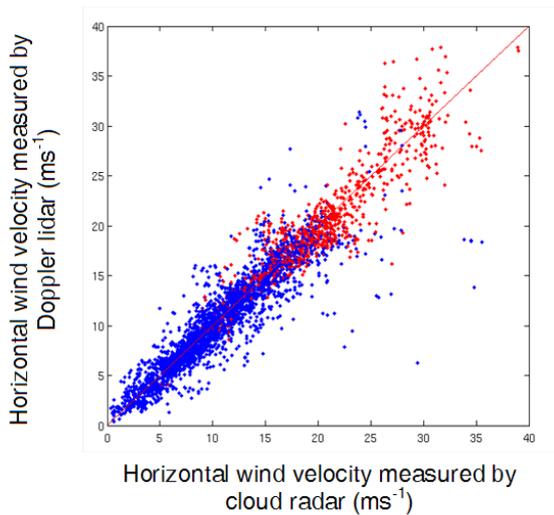

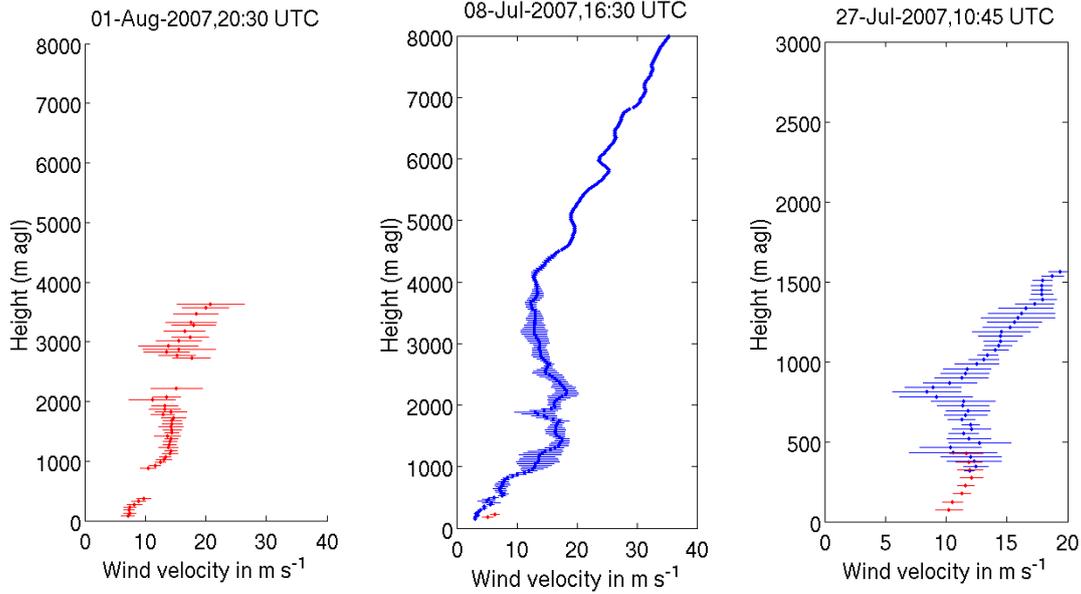Figure 2: Same as Figure 1, but clutter corrected.

Figure 3: Combined profiles from lidar (red) and radar (blue) under optimum conditions for lidar (left), radar (center) and changing conditions with height resulting in a complementary profile (right)

is shown in Figure 4. The highest absolute frequencies of vertical wind speed is found in the range of $\pm 1 \ ms^{-1}$ around the 1:1 line. Upward velocities reach up to $3 \ ms^{-1}$ for both instruments, downward velocities to $-8 \ ms^{-1}$. A ground clutter problem is visible along an axis of zero radar velocity. Figure 4 shows a large amount of strong downward radar velocities whereas lidar velocities are close to zero. For further evaluation the simultaneously measured velocities are attached to different atmospheric situations. A critical lidar backscatter value was empirically determined and used to identify measurements within clouds. A threshold radar reflectivity of 0 dB at a height of 500 m agl is applied to identify rain, since 0 dB corresponds to a rain rate of around $0.01 \ mmh^{-1}$.

4.1 Clear air measurements

If the cloud and the rain criteria are not fulfilled, the situation is defined as clear air situation. Figure 5 shows the frequency distribution of the measured differences. High values of absolute frequency along a vertical axis of lidar velocities around $0 \ ms^{-1}$, could be interpreted as falling scatterers (e.g. light rain), which were not detected by the threshold. Nevertheless 76% of the simultaneously measured velocities differed by less than $\pm 1 \ ms^{-1}$ and 25% by less than $\pm 0.1 \ ms^{-1}$. 75% of the range gates show identical wind direction (both instruments measured upward or downward wind). When only velocities of more than $0.2 \ ms^{-1}$ are taken into account, the value of agreement reached 90%.

A clear air day was analyzed additionally to exclude rain or cloud effects completely. Now 95% of the valid measurements differed less than $1 \ ms^{-1}$ and 40% less

than $\pm 0.1 \ ms^{-1}$. To evaluate vertical velocities and possibly associated turbulence, it is necessary to find suitable situations through a robust criteria excluding all kinds of precipitation.

4.2 Lidar double peaks and rain drop distribution

The different velocities measured by lidar and radar due to the different detectable scatterers sizes can be used to estimate scatterer size distributions. This can be shown by analyzing rain events, which were connected with high velocity differences. Figure 6 shows simultaneously measured data fulfilling the rain criteria. Two clusters of data are obvious: along and especially slightly below the 1:1 line and along a vertical line of nearly zero lidar velocity. This distribution is explainable from the lidar Doppler spectrum (Figure 7), where double peaks appeared during rain events . In these cases the peak at the minimum frequency could be interpreted as the velocity of falling rain drops, the second peak, which is generally located around $0 \ ms^{-1}$, as the velocity of the air. Depending on the relative size of the two peaks, the air or the rain peak is identified by the automated lidar algorithm. Using a 2-component Gauss model as proposed by Lottman et al. (2001)

$$fit = a_1 \cdot e^{\left(-\frac{(x-b_1)^2}{2c_1^2}\right)} + a_2 \cdot e^{\left(-\frac{(x-b_2)^2}{2c_2^2}\right)} + a_3 \quad (5)$$

the two regions, shown in Figure 6, can be separated.

The mean velocity from the radar data was by $3.0 \ ms^{-1}$ lower than the velocity from the lidar during precipitation (modal $0.6 \ ms^{-1}$). This difference is used to calculate raindrop size distributions approximately.

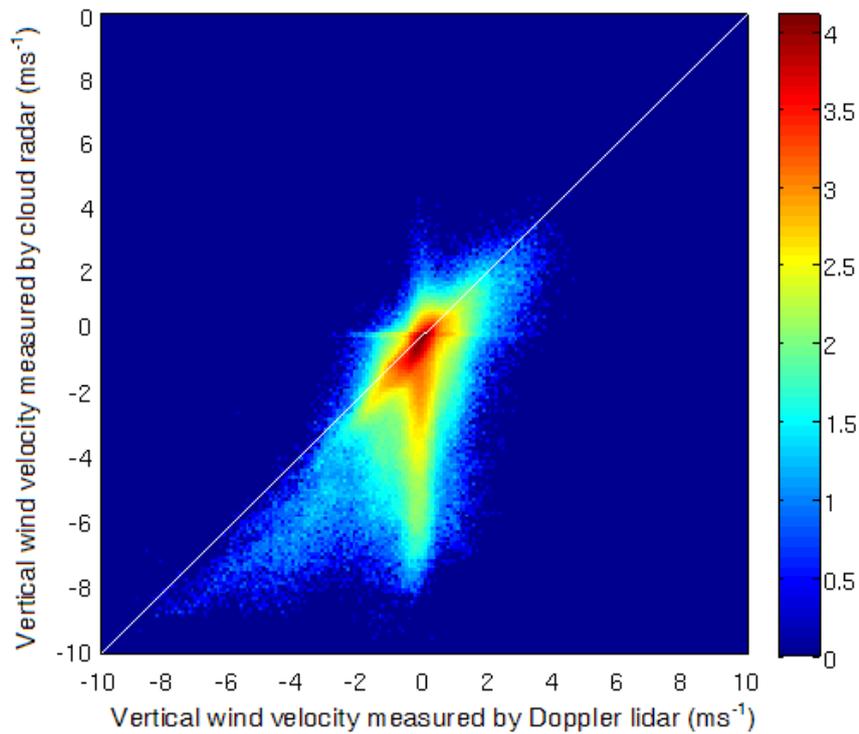Applying the empirical formula of Atlas et al. (1973)

4

Figure 4: Absolute frequency of simultaneous measured vertical velocities. The plot is scaled logarithmic (2 corresponds to $10^2 = 100$) , the intervals are $0.1\ ms^{-1}$. Each pixel is colored according to the amount of simultaneous measured velocities, e.g. f(-1,-4)=66 (log66=1.8) corresponds to a total number of 66 time-height-range-gates joint to a lidar velocity of $-1\ ms^{-1}$ and a radar velocity of $-4\ ms^{-1}$.
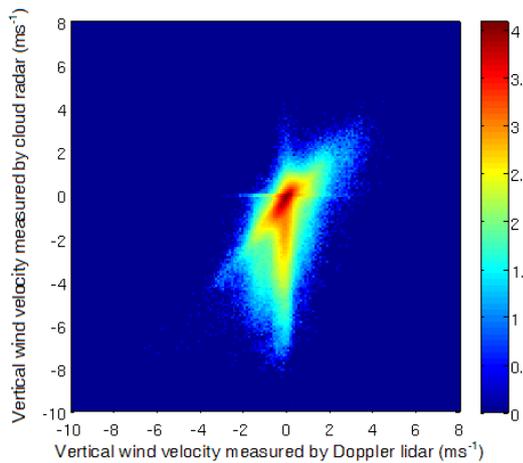

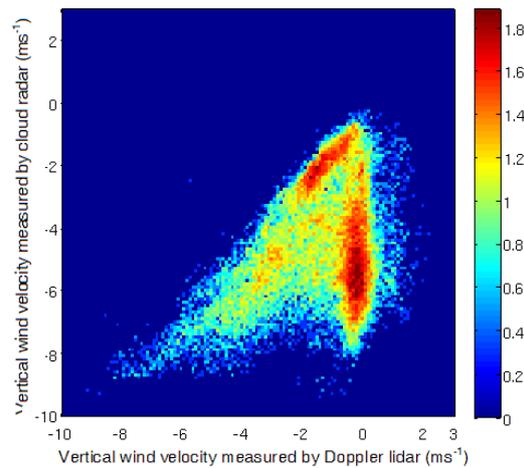Figure 5: Same as Figure 4, but no cloud or rain criteria and modified axis ranges

Figure 6: Same as Figure. 4, but rain and no cloud criteria and modified axis ranges
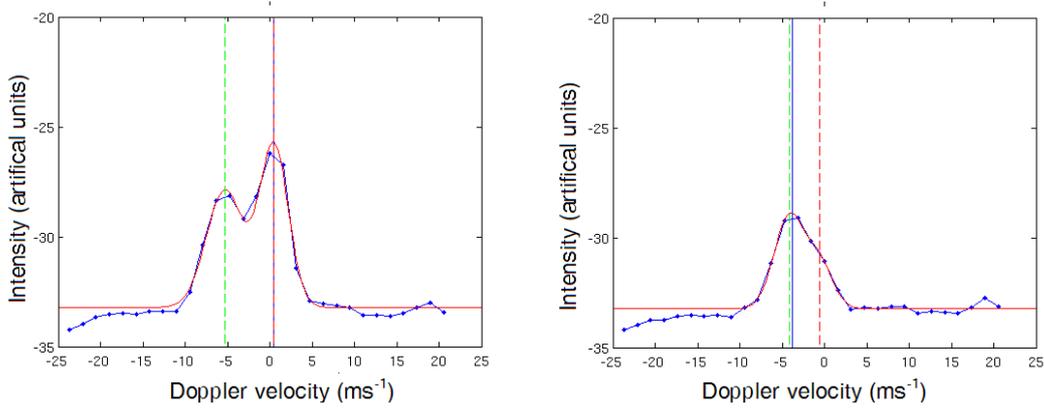
Figure 7: Doublepeaks in the Doppler spectrum during rain events (blue) and the fit of a 2-component Gauss model (red); left: air peak is identified by lidar algorithm (blue vertical line); right: rain peak is identified

for terminal fall velocity

$$v(D) = 9.65\ ms^{-1} - 10.3\ ms^{-1} \cdot e^{(-0.6\ mm^{-1}\ D)} \quad (6)$$

and a Gamma distribution (parameters N_0, μ and λ) for the number density of rain drop size

$$N = N_0 \cdot D^{\mu} \cdot e^{(-\lambda D)} \quad (7)$$

the radar and lidar velocities are calculated from equation 1 to 4 according to

$$v_{Radar} = 9.65 - 10.3 \frac{\lambda^{\mu+7}}{(\lambda + 0.6)^{\mu+7}} \quad (8)$$

$$v_{Lidar} = 9.65 - 10.3 \frac{\lambda^{\mu+3}}{(\lambda + 0.6)^{\mu+3}} \quad (9)$$

Fall velocities from lidar and radar were corrected for air velocity and averaged over the lowest 750 m above ground. The solid line in Fig. 8 (bottom) shows the rain drop size distribution for a 5 minutes rain episode. A satisfying agreement between the calculated distribution and a measured one using a collocated distrometer, was observed (bars in Fig. 8 , bottom). Nevertheless there are limitations: the raindrops have to reach their terminal fall velocity to apply the algorithm correctly. Lidar measurements during rain are still rare, and the velocities from radar and lidar must be measured very accurate to get the minor differences between rain spectra .

4.3 Power spectra

Power spectra and profiles of the vertical velocity variance have proven to be useful tools in turbulence research (Frehlich et al., 1998). The last two sections addressed the range of differences in vertical velocity measurements. Power spectra are analyzed to see if the vertical velocity variance is influenced by these differences and to figure out the possibilities of getting complementary variance profiles using the instrument combination.
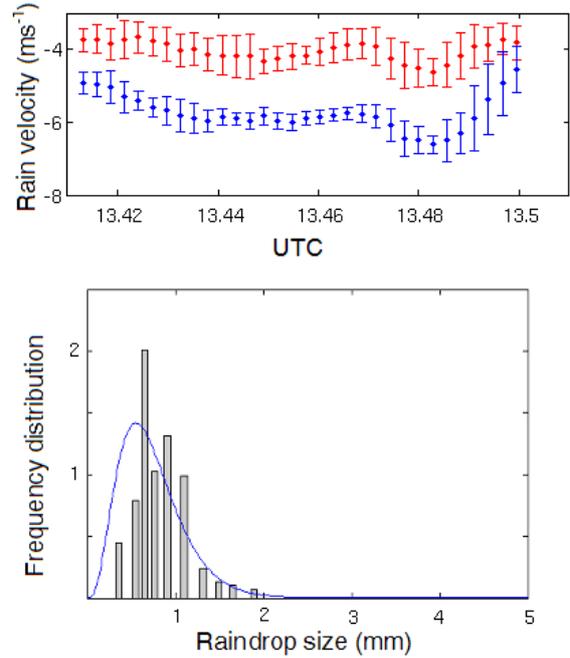

Figure 8: Different velocities measured by lidar (red) and radar (blue) (top) and the measured raindrop size distribution from distrometer (bars) and calculated from velocity difference (curve) (bottom).

The classical discrete Fourier transformation to calculate spectra could not be applied usefully due to the COPS scan strategy, which comprised 5 minute data gaps within each 30 minutes period. A periodogram is calculated via a least square fit instead

$$v_t - \overline{v} = \beta_1 * cos(2\pi\lambda t) + \beta_2 * sin(2\pi\lambda t) \quad (10)$$

with vertical velocity v_t, temporal mean $\overline{v}$ and $\lambda \in [0, 0.5]$. The components of the periodogram are calculated from the estimators $\tilde{\beta}_1$ and $\tilde{\beta}_2$ according

$$I(\lambda) = \frac{1}{4} * N * (\tilde{\beta}_1^2 + \tilde{\beta}_2^2) \quad (11)$$

$$\sigma_w^2 = \sum_{\lambda=-0.5}^{0.5} I(\lambda) * \Delta\lambda = \sum_{\lambda=0}^{0.5} 2 * I(\lambda) * \Delta\lambda \quad (12)$$

An additional factor N/N* (with number of available measurements N* and N number of theoretically possible measurements without data gap) is used, to address the data gap. For time steps of 1 minute, periodograms using data of 60 minutes time intervals were calculated. The variances calculated from the periodogram are consistent with statistical variances directly from the data. For intercomparison the spectra are smoothend by averaging over 60 spectra. Figure 9 shows an early afternoon spectrum under clear air convective conditions. The cut-off frequencies differed because if the different time resolutions of the radar and the lidar. In general the spectra behave quite similar. They show a $-\frac{5}{3}$ slope in the inertial subrange.

Figure 10 shows differences observed in spectra from rain events. In these cases the radar measurements showed significantly higher values at low frequencies. This is related to a higher radar vertical velocity variance.

Because of the short presence of moving clouds over among the instruments, the used method is not applicable to investigate the behavior of the spectra in convective clouds.

5 Conclusions

Using the very large COPS data set, covering European summer conditions, with coordinated measurements of a scanning 35.5 GHz cloud radar and a scanning $2 \ \mu m$ Doppler lidar, the possibilities of combined measurements are investigated. Due to the different wavelengths of the instruments and resulting sensitivity to different scatterers, the combination led to a higher data availability in space and in time.

Vertical profiles of horizontal wind velocity and wind direction could be measured through the boundary layer and through clouds. For 150 measurement hours covering day and night and different weather conditions, the total number of valid data compared to single lidar measurement was increased by a factor of 1.6 by combining both instruments. This is equivalent to 50%

of data availability. This significant increase underlines the potential of joint horizontal wind measurements.

The coverage of vertical wind velocities measured in vertical stare operation in the lowest 2 km increased by a factor of 1.7 compared to single lidar measurements. Differences between the velocities occurred, but could be explained by size-dependent fall velocities of the scatterers. During rain events the Doppler spectra of lidar data showed double peaks. The different rain velocities measured by lidar and radar are used to estimate rain drop size distributions. Comparisons to measured distributions showed satisfying results. Much higher velocity resolution is needed to measure small variations in the distributions.

Power spectra under convective conditions show good agreement. This could give the opportunity to extend variance spectra into clouds. In order to do that further research is needed.

References

D. Atlas, R. C. Srivastava, and R. S. Sekhon. Doppler Radar Characteristics of Precipitation at Vertical Incidence. *Reviews of Geophysics and Space Physics*, 11, Feb. 1973.

K. Browning and R. Wexler. The determination of kinematic properties of a wind field using doppler radar. *Journal of Applied Meteorology*, 7:105 –113, 1968.

R. Frehlich, S. M. Hannon, and S. Henderson. Coherent doppler lidar measurements of wind field statistics. *Boundary-Layer Meteorology*, 1998.

J. Handwerker and U. Görsdorf. Wind profiles generated with a scanning cloud radar. *Proceedings of the 4th European Conference on Radar in Meteorology and Hydrology*, 2006.

B. Lottman, R. Frehlich, S. Hannon, and S. Henderson. Evaluation of vertical winds near and inside a cloud deck using coherent doppler lidar. *Journal of Atmsopheric and Oceanic Technology*, 18:1377–1386, August 2001.

V. Wulfmeyer, A. Behrendt, H. Bauer, C. Kottmeier, U. Corsmeier, A. Blyth, G. Craig, U. Schumann, M. Hagen, S. Crewell, P. D. Girolamo, C. Flamant, M. Miller, A. Montani, S. Mobbs, E. Richard, M. Rotach, M. Arpagaus, H. Russchenberg, P. Schlüssel, M. König, V. Gärtner, R. Steinacker, M. Dorninger, D. Turner, T. Weckwerth, A. Hense, and C. Simmer. Research campaign: The convective and orographically induced precipitation study. *Bull. Amer. Meteor. Soc.*, 2008.
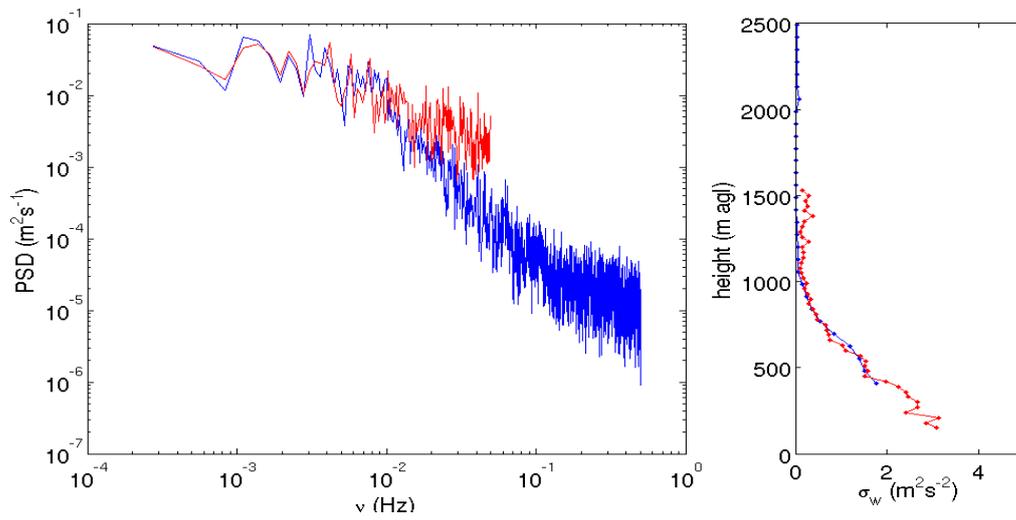
Figure 9: Power spectra calculated over 60 minutes data intervals and averaged over 60 spectra (left) and the vertical velocity variance as the integral over the whole spectra (right), data measured during clear air, convective conditions
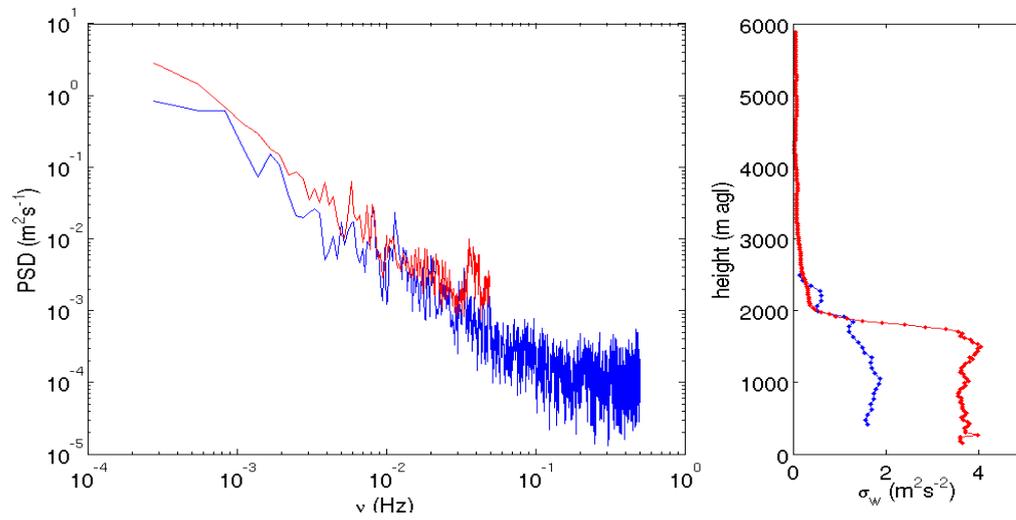

Figure 10: Same as 9, but data measured during rain.